Available online at www.sciencedirect.com
SCIENCE DIRECT®
C. R. Physique 6 (2005) 921–933
COMPTES RENDUS PHYSIQUE
http://france.elsevier.com/direct/COMREN/

Spintronics/Spintronique

Magnetism in reduced dimensions

Olivier Fruchart [a,*], André Thiaville [b]

[a] *Laboratoire Louis-Néel (CNRS), 25, avenue des Martyrs, BP166, 38042 Grenoble cedex 9, France*
[b] *Laboratoire de physique des solides, université Paris-Sud, bâtiment 510, 91405 Orsay cedex, France*

Available online 7 December 2005

Abstract

We propose a short overview of a few selected issues of magnetism in reduced dimensions, which are the most relevant to set the background for more specialized contributions to the present Special Issue. Magnetic anisotropy in reduced dimensions is discussed first, on a theoretical basis, then with experimental reports and views from surface to single-atom anisotropy. Then, conventional magnetization states are reviewed, including macrospins, single domains, multidomains, and domain walls in stripes. Dipolar coupling is examined for lateral interactions in arrays, and for interlayer interactions in films and dots. Finally thermally-assisted magnetization reversal and superparamagnetism are presented. For each topic we have sought a balance between well established knowledge and recent developments. ***To cite this article: O. Fruchart, A. Thiaville, C. R. Physique 6 (2005).***

Résumé

Magnétisme en dimensions réduites. Nous proposons un panorama de quelques aspects du magnétisme en dimensions réduites, appropriés comme toile de fond pour les articles plus spécialisés de ce numéro spécial. L'anisotropie magnétique en dimensions réduites est discutée, sur le plan théorique, puis appuyée par des exemples, allant des surfaces aux atomes individuels. Les configurations d'aimantation les plus courantes sont ensuite décrites : macrospins, monodomaines, multidomaines, parois dans des bandes. Les couplages magnétiques, essentiellement dipolaires, sont décrit pour des réseaux et pour des bi-couches. Enfin nous présentons les effets de l'activation thermique, de la baisse de coercitivité jusqu'au superparamagnétisme. Pour chaque aspect nous avons recherché un équilibre entre résultats établis et développements récents. ***Pour citer cet article : O. Fruchart, A. Thiaville, C. R. Physique 6 (2005).***

Keywords: Nanomagnetism; Micromagnetism; Magnetic anisotropy; Superparamagnetism; Reduced dimensions

Mots-clés : Nanomagnétisme ; Micromagnétisme ; Anisotropie magnétique ; Superparamagnétisme ; Dimension réduite

1. Introduction

Magnetism in reduced dimensions has been an active topic in the last two decades. Much progress, still under way, has been made possible by the conjunction of three aspects. First, the progress of fabrication techniques, both deposition and lithography. Second, the progress of magnetic characterization techniques like XMCD and XMLD, Lorentz microscopy, SEMPA,

* Corresponding author.
E-mail addresses: Olivier.Fruchart@grenoble.cnrs.fr (O. Fruchart), thiaville@lps.u-psud.fr (A. Thiaville).

1631-0705/$ – see front matter
doi:10.1016/j.crhy.2005.10.011

XMCD/XMLD-PEEM, SPLEEM, sp-STM, magnetic scattering and surface diffraction etc. Third, the considerable increase of computing power. Today, all three aspects overlap in the range 20 nm–1 μm, which makes our era very productive. This length scale could define *nanomagnetism*. A better term might have been *mesomagnetism*, i.e. at the cross-over from macroscopic behaviors to uniform magnetization, although the term 'meso' has not been considered by the community of magnetism.

The interest in nanomagnetism has also been boosted by the discovery of new (or revisiting of) phenomena that arise owing to the fabrication of heterostructures at the nanoscale, and that underlie most of the topics of the Special Issue: giant magnetoresistance, tunneling magnetoresistance, exchange anisotropy and bias, spin torque. In this contribution we review some basic aspects of magnetism in reduced dimensions for mostly single systems, that are useful to consider before implementing some of the above-mentioned effects in complex heterostructures, may it be for realizing functional devices or structures for fundamental investigations. The topics covered are magnetic anisotropy, magnetization states, interactions (mostly dipolar) and thermal activation.

2. Magnetic anisotropy in low dimensions

Here we discuss *microscopic* magnetic anisotropy energy (MAE), a field subject to breaking discoveries in the recent years. Dipolar anisotropy will be treated in Section 3. Other low-dimensional effects are excluded from the discussion, such as magnetic moments at interfaces or the reduction of ordering temperature; see [1–3] for reviews. The former is relevant to spintronics e.g. for the TMR effects, see [4]. The latter is often screened by *superparamagnetism*, treated in Section 5.2.

2.1. Theoretical descriptions

MAE results from the interaction of magnetization with the local environment of atoms, via the crystal electric field [5]. In bulk materials at equilibrium this is the *magnetocrystalline anisotropy* E_{mc}. When any dimension of a system is reduced corrections to E_{mc} arise, due to interface or strain (deformation of the structure).

Long before thin films could be grown epitaxially and at the nanometer scale, Néel foresaw that the local breaking of symmetry at surfaces should induce a correction to E_{mc}, which he named *surface anisotropy* (E_{s}, an energy per unit area) [6]. E_{s} is nowadays often referred to as *Néel surface anisotropy*.[1] He used a pair model to predict the angular variation of E_{s}, the summation being restricted to magnetic neighbors. E_{s} could be expanded in spherical harmonics, although simple polynomial expansions are more popular, with the most simple form being uniaxial anisotropy: $E_{\mathrm{s}} = K_{\mathrm{s}} \cos^2\theta$. In a crude approximation, numerical coefficients were derived from magnetoelastic coupling coefficients, yielding values around 0.1–1 mJ/m^2 ∼ 0.1–1 meV/atom, surprisingly of the correct experimental order of magnitude, 0.1 mJ/m^2 as revealed experimentally much later. It is commonly acknowledged today that this model fails to predict exact figures, even their sign, which can only be derived from experiments or ab initio calculations.

A more rigorous view of surface anisotropy than Néel's was given by Bruno, who predicted the proportionality of surface anisotropy constants with the anisotropy of the angular momentum [7]. To understand this fact, it should be recalled first that in a bulk 3D solid the orbital momentum is very nearly zero, as the electron wavefunctions loose the rotation invariance that exists in the atom, because of the crystalline electric field. As a result, the angular momentum in bulk 3D is very small compared to the spin moment, and in fact appears only as a perturbation when including the spin-orbit term. At a surface or interface however, the crystalline electric field has a reduced symmetry and becomes compatible with a perpendicular orbital moment. This induces, via the spin-orbit coupling, an extra MAE. The initial model of Bruno [7] was based on a tight binding approach of the electronic structure in a 3D transition metal atomic layer (AL), and has been refined later [8]. More realistic ab initio calculations have revealed some departures from this general trend [9].

2.2. Thin films, a model for surface anisotropy

Thin epitaxial films are model systems. The translation symmetry in-the-plane yields a laterally-small unit cell, at reach to ab initio computation, and easing experimental analysis. Close-to-ideal films are nowadays routinely fabricated for many systems, which can be controlled down to the single AL.

The first clear confirmation of the existence of E_{s} was given by Gradmann et al. in the late 1960s [10]. The total uniaxial MAE $E = K_{\mathrm{tot}}(t)\cos^2\theta$ of $Fe_{52}Ni_{48}$/Cu(111) films of thickness t followed a $1/t$ dependence, the slope being ascribed to E_{s}: $K_{\mathrm{tot}}t = K_{\mathrm{bulk}}t + 2K_{\mathrm{s}}$. Notice that K_{bulk} includes both magnetocrystalline anisotropy and shape anisotropy $K_{\mathrm{d}} = \frac{1}{2}\mu_0 M_{\mathrm{s}}^2$,

[1] Notice that this pioneering approach [6] already included the dipolar contribution to E_{s}, arising from the discrete location of magnetic moments. This effect is covered and extended in Ref. [151].

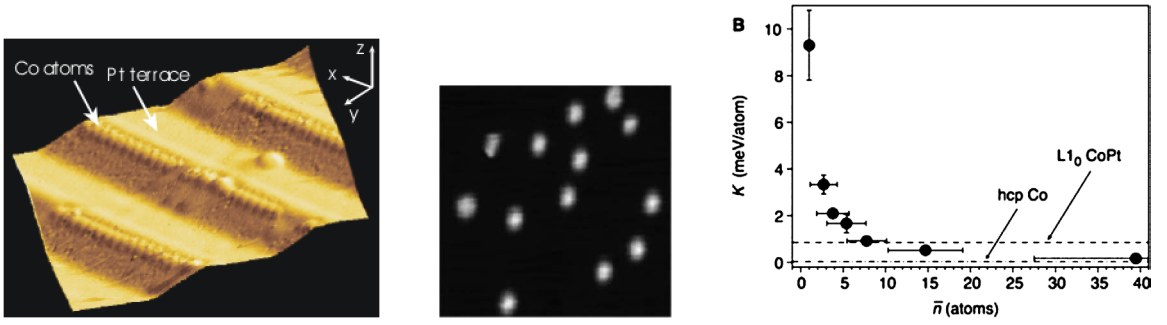

(a) (b) (c)

Fig. 1. (a) Monoatomic Co wires decorating steps of Pt(997) [30]; (b) Single Co atoms on Pt(111) [31]; (c) perpendicular MAE for Co/Pt(111) as a function of the cluster size.

θ being the angle of magnetization with the normal to the film plane. These experiments, performed down to a few ALs, first suggested the possibility to attain an effective *perpendicular anisotropy*, provided that K_s is negative and sufficiently large to overcome K_d for a few atomic layers. Examples of perpendicular anisotropy are Au/Co/Au, Pt/Co/Pt and Pd/Co/Pd (multi)layers, with critical thicknesses for spin reorientation transition in the range 1–2 nm.

It was then realized [11] that $1/t$ plots mix surface K_s and magnetoelastic K_{mel} contributions. Indeed structural models predict at equilibrium a $1/t$ relaxation of strain $\bar{\bar{\epsilon}}$ in heteroepitaxial growth [12,13] so that $K_{mel} \sim 1/t$. Thus true K_s values could only be extracted after subtraction of K_{mel} when $\bar{\bar{\epsilon}}$ is measured and magnetoelastic coefficients B_{mel} are known, or in the more rare case of pseudomorphic growth over a range of many ALs, like for Ni/Cu(001) [14]. K_s values obtained in this fashion are reviewed in [1].

More recently, the direct measurement of E_{mel} in films using bending cantilevers, and the revisiting of previous data, revealed that E_{mel} is no more linear with $\bar{\bar{\epsilon}}$ in ultrathin films [15–18]. Higher order terms in ϵ need to be considered, which e.g. for Fe can reverse the sign of B_{mel} at less than 1% of strain [16]. This had been overlooked in bulk samples because plastic deformation occurs well below the strain values commonly observed in heteroepitaxial films. The re-entrant in-plane magnetization of Ni/Cu(001) in the ultrathin range [17,19], is now explained by non-linear magnetoelastic effects. The strain dependence of K_s itself was also postulated, initially on Ni/Cu(001) [20], however of puzzlingly high magnitude, and could never be confirmed unambiguously. From all this it must be concluded that magnetoelastic and true Néel-type anisotropy are entangled in thin films. Their clear separation, even conceptually, is impossible in most systems, where only an effective K_s can be deduced from $1/t$ plots.

On the microscopic level several experiments (see Ref. [21] for the pioneering work) have confirmed the link between MAE and the anisotropy of the orbital momentum, using magnetic circular dichroism effects with soft X rays (XMCD). The anisotropy of the orbital momentum for 3D elements at surfaces is of the order of 0.1 μ_B/atom.

2.3. Surface anisotropy in nanostructures

Beyond the model case of thin films, surface anisotropy applies to all atoms located at the surface of any nanostructure. The length scales of the physical effects giving rise to E_s are in the low nanometer range, and the atomic arrangement close to the interface is crucial, so that nanostructures fabricated by lithography or by any other artificial mean are not adequate to evidence E_s in reduced lateral dimensions. Instead, when this field has been explored in the last decade, one used e.g. clusters fabricated by physical means [22], or epitaxial self-organization (SO) at surfaces [23,24]. The disentanglement of magnetoelastic and true Néel anisotropy is even more difficult than for thin films, given the complexity of geometry and strain, and *in most cases* because of the distribution of local environments (loss of the small unit cell). Therefore, in the following we should consider E_s as an *effective* surface anisotropy, without trying to discuss its physical origin.

Notice that in nanostructures such as those discussed above, the local reduction of dimensionality can be more severe than at the 2D surface of thin films, i.e. with a higher loss of coordination. Epitaxial growth was then used for its ability to produce nanostructures with a more monodisperse type of interfacial atoms than for clusters, to analyze quantitatively the concepts of *edge anisotropy* for a 1D interface (e.g. an atomic edge, or the edge of a monolayer-high island), or even *kink* anisotropy for a 0D defect along such a 1D interface, or an isolated magnetic atom on a surface, as we will see. Pioneering work was performed on ultrathin films grown on *vicinal* surfaces, giving rise to a regular array of stepped sites [25,26]. After correction for the tilt of crystal axes for E_{mc}, a clear linear variation of anisotropy with the miscut angle can be evidenced, and interpreted as a *step* anisotropy with a magnitude of the order of 1 mJ/m^2. Later, SO nanostructures have been used to further decrease the

Table 1
Orbital momentum and magnetic anisotropy energy (MAE) of Co atoms on Pt as a function of coordination (after [30,31])

	bulk	mono-layer	bi-atomic wire	mono-atomic wire	two atoms	single atom
Orbital momentum (μ_B/at)	0.14	0.31	0.37	0.68	0.78	1.13
MAE (meV/at)	0.04	0.14	0.34	2.0	3.4	9.2

dimensionality. They were mainly studied with X-ray magnetic circular dichroism (XMCD), for its sensitivity and ability to yield the orbital momentum and its anisotropy. Upon sub-AL deposition on the vicinal surface Pt(997), 1 AL-high Co stripes of adjustable width were fabricated by step decoration [27] (Fig. 1(a)). A surface-RKKY-type of variation of the MAE was evidenced, oscillating with the width of the stripes [28,29] and culminating for monoatomic wires to 2 meV/atom [30]. Minute amounts of Co were also deposited around 15 K on Pt(111), remaining as individual atoms because surface diffusion is frozen at this temperature (Fig. 1(b)). A giant MAE of 9 meV/atom was measured. Upon annealing, Ostwald ripening sets in, yielding islands of well-controlled size and narrow size distribution. Thus, for Co in contact with Pt the variation of MAE from single atoms to bulk was fully spanned for the first time [31,32] (Fig. 1(c)).[2] These studies confirm that the magnitude of E_s increases dramatically from surfaces, to steps, then to kinks or atoms. Besides, while the MAE was derived directly from the fit of XMCD hysteresis curves, the orbital moment was also measured, showing a similar increase for decreasing dimensionality. A reasonable linear variation of MAE with the *anisotropy* of the orbital momentum is found following the simple arguments from Bruno [7]. Ab initio calculations of clusters have also shown this trend [33]. Finally, notice the sharp decrease as a function of size concerning orbital momentum and MAE: a bi-atomic island behaves closer to an infinite monoatomic-wide wire than to a single atom, and bi-atomic wires are closer to a monolayer film than to a mono-atomic wire, see Table 1. For 3D clusters (≈ 3 nm) elaborated in the gas phase and measured individually (see Section 3.2), the careful analysis of the measured MAE has shown that surface terms also dominate [34].

3. Magnetization states and magnetization processes in single systems

3.1. Basics of micromagnetism

A general introduction to the micromagnetic theory should be sought elsewhere [35]. Here we discuss a few selected issues only.

Demagnetizing coefficients and magnetic length scales are useful parameters to discuss magnetization patterns. It can be shown [36] that a demagnetizing tensor $\overline{\overline{\mathbf{N}}}$ can be defined for a sample of *arbitrary* shape *assumed* to be uniformly magnetized:

$$\left\langle \mathbf{H}_d(\mathbf{r}) \right\rangle = -\overline{\overline{\mathbf{N}}} \cdot \mathbf{M} \tag{1}$$

with $\mathbf{M}$ the magnetization vector and $\langle \mathbf{H}_d(\mathbf{r}) \rangle$ the demagnetizing field *averaged* over the sample. The density of demagnetizing energy is immediately $E_d = -\frac{1}{2}\mu_0 \langle \mathbf{H}_d(\mathbf{r}) \rangle \mathbf{M}$. $\overline{\overline{\mathbf{N}}}$ is positive and symmetric, thus can be diagonalized, so that along any main axis i, one has $\langle \mathbf{H}_d(\mathbf{r}) \rangle = -N_i \mathbf{M}$. It can be shown that $\mathrm{Tr}\,\overline{\overline{\mathbf{N}}} = 1$, so that $\sum_{i=1}^{3} N_i = 1$. The emphasis is often put on samples bounded by surfaces of polynomial equations not greater than two (of practical interest are thin films – also called slabs, ellipsoids, infinite cylinders with elliptical cross-section). Only in these is $\mathbf{H}_d$ uniform if $\mathbf{M}(\mathbf{r}) \equiv \mathbf{M}$, so that Eq. (1) is valid at any point and the uniformity of $\mathbf{M}(\mathbf{r})$ can be practically achieved along the main axes for $|H_{ext}| \gtrsim N_i M$. Analytical formulas for N_i's can be found for revolution ellipsoids [37], prisms [38,39] (Fig. 2), cylinders of finite length [40–42], and tetrahedrons [43,36]. For other geometries micromagnetic codes or Fourier-space computations [36] can be used.

Characteristic magnetic length scales arise in non-homogeneous magnetization structures resulting from the competition between two (or more) types of energy. The competition of exchange A and anisotropy K yields the so-called Bloch wall width $\Delta = \sqrt{A/K}$ for the case of uniaxial anisotropy. Δ is relevant to describe the width of walls when E_d is negligible, e.g. in the bulk or in ultrathin films of high anisotropy. The various definitions of the wall width are reviewed in [35], p. 219. The competition of exchange and dipolar energy yields the so-called exchange length $\Lambda = \sqrt{A/K_d}$ with $K_d = \frac{1}{2}\mu_0 M_s^2$. Λ is for instance a measure of the diameter of the core of magnetic vortices in flux-closure patterns. One also defines the dimensionless *quality factor* $Q = K/K_d$. This films of materials with perpendicular magnetocrystalline anisotropy support fully perpendicular domains under zero external fields for $Q > 1$ (stripes and bubbles for low coercivity, up to fully remanent for coercive materials), and continuously rotating structures for $Q < 1$ (weak, strong stripes).

[2] Previous pioneering studies were reported, although incomplete in terms of spanning of dimensionality, see [152,153,144,154].

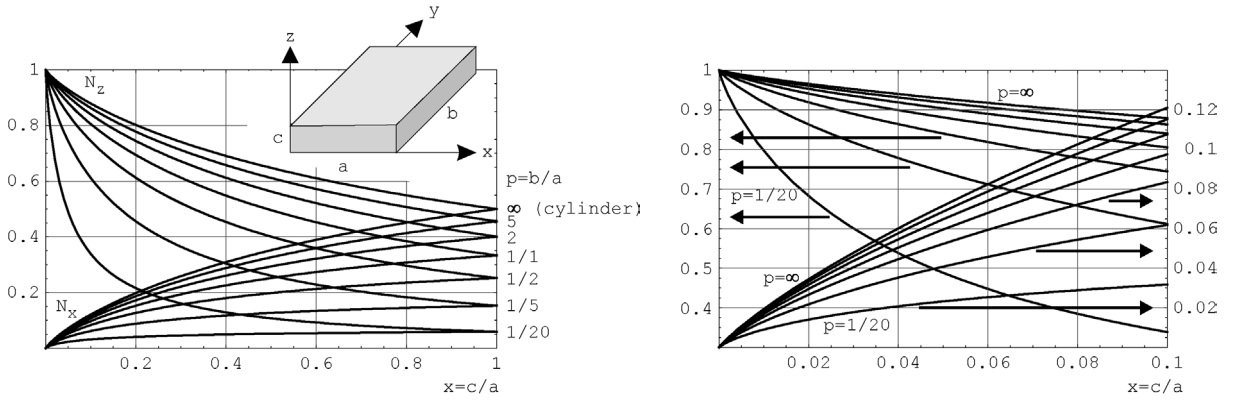

(a) (b)

Fig. 2. Demagnetizing coefficients of prisms: (a) arbitrary shape; (b) close-up view for flat prisms.

3.2. Macrospins

In particles of extremely small size the exchange energy dominates over all other energy terms so that the magnetization state is always nearly uniform even during magnetization reversal, which proceeds by *coherent rotation* of all magnetic moments. This occurs for dimensions of the order or below Λ, $\simeq 10$ nm for common materials like 3d magnetic metals. The particle can then be reasonably described by a single magnetic moment, the so-called *macrospin*, subjected to an effective MAE that gathers the contributions from crystalline, surface and shape anisotropies. The seminal paper investigating the magnetization reversal of macrospins [44], still used intensely, predicts that magnetization reverses by reversible rotation and irreversible jumps, the latter occurring at field values that depend strongly on the field angle with respect to that (those) of the effective anisotropy. This model, initially developed for a uniaxial anisotropy of degree 2, was recently generalized to arbitrary anisotropy [45].

Experiments on individual nanoparticles of decreasing size, mainly performed by Wernsdorfer with a technique called micro-SQUID [46], have beautifully shown this behavior. The anisotropy was revealed by the surfaces (in the space of the applied fields) where a jump occurs, known generally as astroid [47]. The measurements have been extended to dynamics. In the slow regime dominated by thermal agitation, the magnetic relaxation was shown to involve only one time constant at small sizes, whereas at larger sizes a non-exponential relaxation had been observed [48]. The former corresponds to the thermodynamic model of a particle in the macrospin approximation, called Néel–Brown model [49], see Section 5.1. In the fastest regimes in which magnetization precession is important, i.e. $t \lesssim 1$ ns, it was shown that the application of pulses of radio-frequency (rf) fields could decrease the switching field of the particle if of the right frequency [50], pointing to a non-linear resonance effect, i.e. the precession of the macrospin driven by the rf field.

3.3. Single domain states

In-between the macrospin state and a macroscopic state where magnetic domains separated by domain walls occur, lies the so-called *single-domain state*. A single-domain state may be defined by a state close to uniformly magnetized 'on the average', i.e. displaying no magnetic wall nor vortex. The multidomain-to-single-domain transition was predicted long ago [51] through a comparison of the magnetostatic energy of a uniformly magnetized particle (proportional to its volume) to the wall energy of a multidomain state (proportional to the particle surface). The distinction between macrospin and single domain was introduced early, and some analytical estimates of both sizes obtained [52]. For finite size and definite shapes, a number of 'phase diagrams' have been computed, that predict the magnetic structure of minimum energy as a function of sample dimensions or anisotropy, for cubes [53,54], disks [55], squares [56], rectangles [57]. They all show that the single domain state is reached at small sizes and large anisotropy, as expected.

The term 'single domain state' should not be confused with 'uniform magnetization'. In single domain states, although walls and vortices are not found at equilibrium, they may occur during magnetization reversal through complex nucleation-propagation mechanisms. The critical sizes for single-domain and macrospin are comparable for 3D compact particles, however the former may by far exceed Λ for high aspect ratios, like for thin flat dots. These dots correspond to the majority of the small magnetic samples produced by the 'top–down' approach, hence their detailed study in the recent years. We mentioned in Section 3.1 that only for samples shaped as surfaces of degree $\leqslant 2$ is $\mathbf{H}_\mathrm{d}(\mathbf{r})$ uniform when the magnetization distribution is so. For any other shape $\mathbf{H}_\mathrm{d}(r)$ is in general not uniform, so that strictly speaking uniform magnetization cannot be achieved for whatever high value of the applied field. The non-uniformity is especially strong for the case of thin and flat elements (including

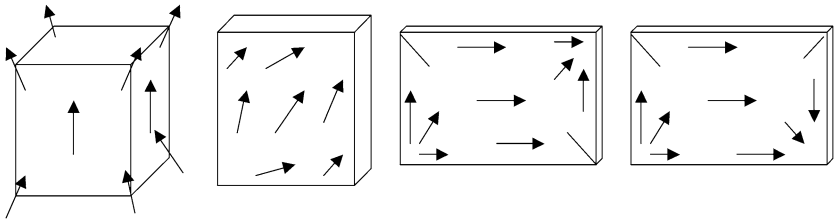

Fig. 3. The most common single domain states (schematic). From left to right: flower, leaf, S and C states.

with in-plane elliptical shape), with a local magnitude that can be considerably higher than the average value, especially close to the edges. The deviations remain down to infinitely small samples [58], where they scale as $(\text{size}/\Lambda)^2$ [59]. The deformations of magnetization linked with the sample shape have been transcribed in the names given to the configurations (Fig. 3).

These deformations are very important as they control the orientation of the average magnetization for magnetically-soft materials, through what has been called the configurational anisotropy [60]. This energy describes the tendency for the magnetization to become non-uniform within the sample so as to decrease magnetostatic energy at the minimum cost in exchange energy. The rigorous computation of this energy requires a special micromagnetics technique called path method [61]. Spectacularly enough, this energy explains how apparent anisotropies of high degree can develop and be measured in triangles, pentagons etc. whereas the conventional shape MAE is only of second degree in magnetization [62]. The magnetization non-uniformity affects also greatly the magnetization reversal. Indeed, the deviations are amplified when a field antiparallel to the average moment is applied. This results in increased switching field and time for switching [63,64] as well as non-coherent reversal processes that may involve vortices [65]. As a consequence, the switching field of even very small samples may differ from the prediction of the macrospin model. Some analytical models have been developed for soft [66] or hard [67,68] magnetic materials. It is, moreover, very likely that these effects are amplified by the surface anisotropy term and the exchange reduction at the surfaces [69,70].

These considerations were limited to perfect samples. The presence of some roughness, especially at the edges of small elements patterned from thin films, was shown to have a big influence on the switching properties [71]. From a magnetostatic point of view, edge roughness increases the energy of a configuration with tangential magnetization. This energy contribution reduces the shape anisotropy, and has been called lateral interface anisotropy [71]. It generally reduces switching fields compared to perfect shapes.

3.4. Confined multidomain states

Multidomain states, also called flux-closure-domain states, have been much studied in the technologically relevant case of thin flat dots made of soft magnetic material like Permalloy. In the limit of vanishing thickness, infinite lateral size and zero MAE, the shape of flux-closure domains is predicted by the Van den Berg's (VdB) construction [72,73], which exhibits charge-free states (notice that, owing to the infinite lateral size, exchange in the domains and the energy of domain *walls* are neglected): magnetic walls are located at the loci of the centers of all disks tangent to the edge of the structure on at least two points. The magnetization vector then lies perpendicular to their radii, i.e. remains parallel to the closest edge (Fig. 4(a), (b)). Configurations of higher order can be obtained by dividing the shape in several equal parts and applying the construction to each of them (Fig. 4(c)). Higher order patterns can result from magnetic history, or arise in the case of moderate in-plane anisotropy to favor domains along easy axis directions. The VdB model was extended under in-plane field [74–76]. All these features were checked experimentally in dots (tens of) microns wide [35]. Surprisingly these models also work reasonably well beyond their theoretical range of validity, i.e. for sub-micron-size, non-soft and rather thick dots, as far as the *center* of the walls is concerned [77–79]. However, a more detailed description at this scale requires the use of micromagnetic theory. This was done analytically e.g. for describing the vortex state in disks [80–82]. Micromagnetic simulations must be used to tackle more complex situations, like the energetics of flux-closure patterns of different orders (see Fig. 4), whose degeneracy in the simple VdB's approach is lifted when the energy of domains walls is rigorously computed [57,83]. Finally, when the thickness of a dot exceeds by far Δ and/or Λ significant variations of magnetization are allowed along the thickness. Such situations provide an interesting intermediate situation between bulk materials that must be described phenomenologically, and thinner and smaller samples that are now understood microscopically. Reports in this field are less common, and include confined stripe domains in perpendicular media [84,85], distorted VdB patterns [86], 3D flux-closure in magnetically-soft cubes [54].

Many experimental, simulation and theoretical reports can also be found on the hysteresis of flux-closure mesoscopic patterns, see e.g. [87,79–81,88,89]. Starting from saturation, flux-closure domains are formed through the nucleation of vortices at the edges. Thus, like for bulk materials, the microscopic details of nucleation remain inaccessible especially because lithography processes often alter the edges in an ill-characterized way. Also, simulated features may sensitively depend on the mesh

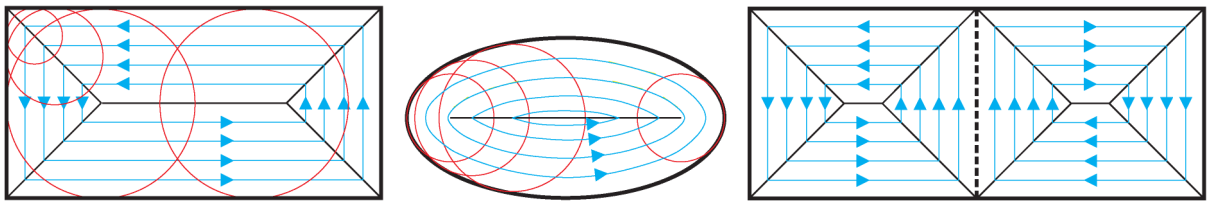

(a) (b) (c)

Fig. 4. Examples of (a), (b) first order and (c) higher order Van den Berg's constructions for flux-closure magnetic states.

used (size, tetrahedrons in finite elements or prisms in finite differences methods, with sometimes spurious effects on tilted edges [90,82]), the order of polynomial interpolation of the various micromagnetic quantities between the nodes of the mesh, the minimization algorithm used (energy minimization or precessional dynamics with damping). Thus, great care is needed in analyzing and comparing nucleation results, because different nucleation events can lead through bifurcation to different flux-closure patterns at zero field [79].

One fundamental interest of confined flux-closure patterns is to benefit from the internal dipolar field of a nanostructure that traps rigidly one or a few vortices and/or wall, and consider these as magnetic objects. These objects can be better studied and manipulated through the application of (possibly strong) external fields while magnetic *domains* remain unaffected. In thin films such fields often move these objects out of the field of imaging and only limited experiments have been reported [91,92]. This includes the stabilization of asymmetric Néel walls at thicknesses well beyond those found in thin films [86], the topological identity of a vortex with a Bloch wall of finite length [77], the compression/expansion [93] and magnetization reversal through Bloch point nucleation [94,95] of vortex' cores under the application of a longitudinal field. The following section reports on further examples of the manipulation of magnetic walls as individual objects, in a semi-confined geometry.

3.5. Magnetic walls in stripes

Samples very long in one dimension but of nanometric size transversally (nanowires, nanostripes, nanotubes) are being intensively studied, both as a challenge to nanofabrication [96–99] as for their properties [100] and applications. Indeed, such structures switch by the motion of one domain wall (DW) with a well-defined velocity. Phase diagrams for the DW structures were also computed and measured [101–103]. For small enough wire transverse dimensions, it was shown that the Bloch wall model [104] could be adapted to these structures, even if they are not at all Bloch walls [100]. One of the spectacular consequences of these various DW structures is the predicted huge velocity difference between two DW structures in cylindrical wires, namely the transverse and Bloch point walls [105]. The dynamics of a DW under a strong current flowing along the wire, due to the spin transfer effect, is now an active subject, both experimentally [106–108] and theoretically [109,110]. Domain walls can also be trapped when the cross-sectional area decreases, a so-called geometrical constriction. When this area decreases steeply enough in the core of the constriction, the wall is compressed. Its width is then predicted to be determined solely by the geometry of the constriction, independently from materials' parameters like exchange [111]. Domain wall compression in nanometer-sized constrictions has been confirmed experimentally [112].

4. Dipolar interactions

4.1. Coupled layers

Two magnetic layers $F1$ and $F2$ separated by a non-magnetic layer N with rough interfaces are coupled through dipolar fields. This situation was first described by Néel, and named *Orange peel coupling* [113]. It was later pointed out that Néel's model was developed for semi-infinite Fi's, whereas for the really thin films studied nowadays a different formula is more adequate [114], predicting a much reduced coupling field H_{N}. This fact is still too often ignored. For vertically-correlated roughness the coupling is positive for in-plane magnetization [114], while for perpendicular magnetization the sign of the coupling depends on geometrical and material parameters [115]. In all cases the coupling decays exponentially with the thickness of the spacer layer.

Bi-(or multi-)layers of finite lateral size, i.e. in the form of dots, are subject to a negative coupling arising from the magnetic poles at the edges of the dot for in-plane magnetization, and a positive coupling for out-of-plane magnetization. For both cases an upper bound for H_{N} arising from $F1$ or $F2$ is $N_1 M_{\mathrm{s},1}$ with N_1 and $M_{\mathrm{s},1}$ the in-plane demagnetizing factor and the magnetization of $F1$, respectively.

Let us examine the consequences of coupling in bilayers [116]. Notice that the physics described below may arise from other types of coupling, like RKKY [117]. The limit of weak coupling is when H_N is smaller than the coercive fields of both layers, $H_{c,1}$ or $H_{c,2}$. In such a case the coupling results in shifted (biased) minor hysteresis loops. Notice however, that even in this weak coupling limit dipolar fields may be locally much more intense than H_N when domain walls occur, like during magnetization reversal [118]. This may lead to progressive demagnetization of the hard layer of spin valves [119] or nucleation of reversed domains in the vicinity of domain walls [120]. In the strong coupling limit H_N is larger than both coercive fields, resulting in rigidly coupled layers. The single-domain limit is shifted upwards for in-plane magnetization in dots because demagnetizing fields are reduced, while it is shifted downwards for out-of-plane magnetized dots. Multidomain states are also affected as the flux be partly closed from one layer to the other, yielding magnetization vectors locally perpendicular to lateral edges.

4.2. Dipole–dipole lateral interactions

Nanostructures are often found in planar networks; see [121] for a review. In the point dipole approximation, an upper bound for the stray field acting at a given site from neighbors closer than radius R and of arbitrary direction of magnetization is proportional to $(\mu_0/4\pi)\int_0^R \frac{2}{r^3} 2\pi r\,\mathrm{d}r \longrightarrow \mathrm{Cte} + \mathcal{O}(1/R)$. Thus dipolar fields are *short ranged* in 2D, contrary to the 3D case. To go beyond the point-dipole approximation one can use analytical formula in the case of spheres or prisms [35], and for more complex shapes micromagnetic codes or a multipole approach [122]. In practice, for a regular network the range of dipolar fields scales with the thickness of the nanostructures, which means first neighbors for e.g. flat dots [123], or many neighbors e.g. in the case of a dense array of elongated cylinders [97]. For perpendicular anisotropy dipolar fields favor checkerboard [124] or stripe patterns [97] depending on the mesh symmetry, e.g. square and hexagonal, respectively. For planar magnetization alternating rows of dots with parallel and antiparallel magnetization directions are favored along an easy axis of the nanostructures in the presence of magnetic anisotropy, or along certain rows of the network in the case of nanostructures magnetically isotropic in-the-plane [125]. Even for weak interactions such states can be approached e.g. through demagnetization procedures. Formalisms and techniques used to characterize couplings include the Preisach model [126], Henkel plots [127,128], or simply shifted minor loops.

5. Thermal effects

5.1. Thermally activated magnetization reversal

On time scales larger than approx. 1 ns the effect of temperature on magnetization processes can be fairly well described by an Arrhenius law proposed by Brown [49] and checked recently against LLG macrospin simulations in the range of tens of nanoseconds [129]: thermal energy allows to overcome an energy barrier ΔE after a waiting time $\tau = \tau_0 \exp(\Delta E/k_B T)$ with $\tau_0 \approx 10^{-10}$ s. The non-trivial issue is to estimate ΔE.

It occurs that for single-domain nanostructures not larger than the domain wall width λ_W (e.g. nanometer-sized clusters [130] and made of soft magnetic material, the macrospin approximation and the Stoner–Wohlfarth model roughly hold *during magnetization reversal* [131]. In the case of uniaxial anisotropy and a field applied along the easy axis we have

$$\Delta E = KV(1 - H/H_a)^2 \tag{2}$$

with $H_a = 2K/\mu_0 M_s$ is the anisotropy field and V the volume of the nanostructure. For a measurement performed over a time duration τ the expected coercivity is

$$H_c(T,\tau) = H_c(T = 0\ \mathrm{K})\left(1 - \sqrt{\frac{k_B T}{KV}\ln\frac{\tau}{\tau_0}}\right) \tag{3}$$

These and other predictions were first confirmed experimentally using single-particle measurements [132]. Notice that in general when H is applied in an arbitrary direction, even close to an easy axis, the dependence of ΔE with H is non-polynomial. The first-order expansion of this dependence defines a generalized exponent α: $\Delta E = KV(1 - H/H_a)^\alpha$, with $\alpha = 1.5$ in most cases [133,134].

For nanostructures larger than λ_W Eq. (2) is not valid, because magnetization reversal if not uniform. One approach consists in replacing V with a so-called *nucleation volume* V_n and considering a phenomenological generalized exponent α. V_n and α may be determined experimentally with temperature- or time-dependent magnetization reversal, the former being sometimes ambiguous because K may vary with T. Besides, time-dependent measurements may be performed at constant field (gate functions with variable duration) or at constant field *variation* (triangle functions). The latter procedure is easier to implement experimentally, however the analysis is more tedious requiring the use of models like Kurkijärvi's [135], which predicts a linear

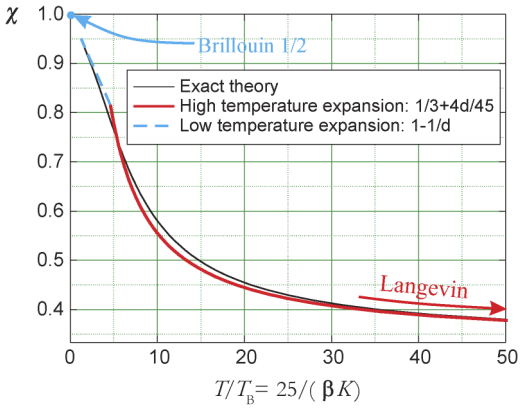

Fig. 5. Exact result and asymptotic expansions for the initial susceptibility of systems with uniaxial second order anisotropy and external field applied along the easy axis direction.

variation of H_c with $\mathrm{d}H/\mathrm{d}t$. Experimentally V_n is often found of size similar to λ_W (λ_W^3 for bulk, $t\lambda_W^2$ for structures of thickness $t < \lambda_W$ etc.), and α is generally in the range 1–2 [123]. $\alpha = 1$ is often found in thin films when domain-wall propagation events determine coercivity; see [136] for a review. Finally notice that deviations from these simple laws are observed when the dynamics are probed over many orders of magnitude. This may arise because of a cross-over, e.g. from propagation- to nucleation-limited coercivity [137]. It has also been proposed that in some cases this may reveal a more complex equation than Eq. (2) with a $1/H$ dependence, explained by the so-called droplet model [138]. Generalized $(1/H)^\mu$ laws were also reported [139] and explained by collective effects. In all theses phenomenological approaches the details of the inhomogeneous magnetization reversal process remain hidden. When full micromagnetic models are available [67,140,141] V_n and α can be evaluated directly, and it is often found that α results from a fit to a non-polynomial variation, so that α is in fact dependent on T and τ.

5.2. Superparamagnetism

Eq. (3) predicts that, for a fixed time scale τ, H_c vanishes for $T > T_B$, with $T_B = (KV/k_B)\ln(\tau/\tau_0)$ being called the *blocking temperature*. This phenomenon is called *superparamagnetism*, in analogy with paramagnetism, however, considering macro-(or *super*)spins. The variation of the time-averaged M with H is generally described by statistical physics using a Boltzmann occupancy law, with the magnetic energy including Zeeman and anisotropy energies. Experimental data in the superparamagnetic regime therefore potentially contain information on the magnetic moment and the anisotropy of the system. However, in most systems, e.g. assemblies of nanoparticles, other parameters interfere like easy axis orientation, interparticle dipolar interactions, and distributions of all these parameters. It is then tricky, or even impossible, to perform a reliable analysis; see [142] for a review.

Quantitative analysis is reliable only when most parameters are known. Let us concentrate on cases with negligible interactions and the external field applied along an easy axis direction. For vanishing anisotropy it is readily derived that the normalized average moment is $m = \mathcal{L}(h)$ with $\mathcal{L}(h) = 1/\tanh(h) - 1/h$ the Langevin function with $h = \mu_0 \mathcal{M} H/k_B T$ and $\mathcal{M}$ the magnetic moment of the system. However, anisotropy cannot be neglected until $T \gtrsim 20T_B$, which is seldom the case in experiments, so that $\mathcal{L}$ should be used with care. For infinite uniaxial anisotropy the Ising case is retrieved: $m = \mathcal{B}_{1/2}(h)$ with $\mathcal{B}_{1/2}(h) = \tanh(h)$ the Brillouin 1/2 function. This case is relevant for self-organized systems with perpendicular anisotropy, which received recently a considerable interest [143–145]. For the real case of finite anisotropy the agreement with the Ising case is satisfactory for $T_B < T \lesssim 5T_B$. An exact expression spans all cases from infinite to vanishing anisotropy [146,147]. Of particular interest for fitting experimental data are the first order expansions of the zero field susceptibility in the low-temperature range ($\chi \sim 1/3 + 4d/45$) and high temperature range ($\chi \sim 1 - 1/d$) with $d = KV/k_B T$ with a cross-over around $T = 5T_B$, which match nearly perfectly the analytical expression [148] (Fig. 5). Notice that we considered temperature-independent material parameters, whereas magnetization, and even more MAE, are expected to decay significantly with temperature in reduced dimensions. This may play a significant or even dominant role, which was not considered here. Dipolar and other interactions can be revealed by an offset in $1/\chi(T)$ plots [143]. The peak in susceptibility measurements can also be used to determine T_B [145].

Let us conclude with some comments. First, the volume relevant for superparamagnetism is always the total volume of the system, not a phenomenological activation volume. Second, superparamagnetism is a drawback for applications in magnetic memory; however, it is an advantage for determining the parameters of the system, provided that a relevant and robust fitting procedure is used, as explained above. Superparamagnetism is also an advantage to prevent aggregation of ferromagnetic nanoparticles in microfluidic or biomedicine [149]. It has also been used in magnetic logic schemes [150].

References

[1] U. Gradmann, Magnetism in ultrathin transition metal films, in: K.H.J. Buschow (Ed.), Handbook of Magnetic Materials, vol. 7, Elsevier Science Publishers B.V., North-Holland, 1993, pp. 1–96 (Chapter 1).
[2] H.C. Siegmann, Surface and 2D magnetism, J. Phys.: Condens. Matter 4 (1992) 8395.
[3] P. Poulopoulos, K. Baberschke, Magnetism in thin films, J. Phys.: Condens. Matter 11 (1999) 9495–9515.
[4] A. Schuhl, Spin-dependent transport (2005).
[5] D. Sander, The magnetic anisotropy and spin reorientation of nanostructures and nanoscale films, J. Phys.: Condens. Matter 16 (2004) R603–R636.
[6] L. Néel, Anisotropie magnétique superficielle et surstructures d'orientation, J. Phys. Rad. 15 (1954) 225–239.
[7] P. Bruno, Tight-binding approach to the orbital magnetic moment and magnetocrystalline anisotropy of transition-metal monolayers, Phys. Rev. B 39 (1989) 865–868.
[8] G. van der Laan, J. Phys.: Condens. Matter 10 (1998) 3239–3253.
[9] P. Ravindran, A. Kjekshus, H. Fjellvøag, P. James, L. Nordström, B. Johansson, O. Eriksson, Phys. Rev. B 63 (2001) 144409.
[10] U. Gradmann, J. Müller, Flat ferromagnetic exitaxial 48Ni/52Fe(111) films of few atomic layers, Phys. Status Solidi 27 (1968) 313.
[11] C. Chappert, P. Bruno, Magnetic anisotropy in metallic ultrathin films and related experiments ion cobalt films, J. Appl. Phys. 64 (10) (1988) 5336–5341.
[12] W.A. Jesser, D. Kuhlmann-Wilsdorf, Phys. Status Solidi 19 (1967) 65.
[13] U. Gradmann, Ferromagnetism near surfaces and in thin films, Appl. Phys. 3 (1974) 161.
[14] R. Jungblut, M.T. Johnson, J. Ann de Stegge, F.J.A. den Broeder, Orientational and structural dependence of magnetic anisotropy of Cu/Ni/Cu sandwiches: Misfit interface anisotropy, J. Appl. Phys. 75 (1994) 6424.
[15] D. Sander, The correlation between mechanical stress and magnetic anisotropy in ultrathin films, Rev. Prog. Phys. 62 (1999) 809–858.
[16] D. Sander, Stress, strain and magnetostriction in epitaxial films, J. Phys.: Condens. Matter 14 (2002) 4165–4176.
[17] K. Ha, R.C. O'Handley, Nonlinear magnetoelastic anisotropy in Cu/Ni/Cu/Si(001) films, J. Appl. Phys. 85 (8) (1999) 5282–5284.
[18] M. Komelj, M. Fähnle, Magnetoelastic effects in ultrathin epitaxial Ni films: an ab initio study, J. Magn. Magn. Mater. 222 (2000) L245–L250.
[19] T. Gutjahr-Löser, D. Sander, J. Kirschner, Magnetoelastic coupling in Ni and Fe monolayers on Cu(001), J. Appl. Phys. 87 (9) (2000) 5920–5922.
[20] G. Bochi, C.A. Ballentine, H.E. Inglefield, C.V. Thompson, R.C. O'Handley, Evidence for strong surface magnetoelastic anisotropy in epitaxial Cu/Ni/Cu(001) sandwiches, Phys. Rev. B 53 (1996) R1729.
[21] D. Weller, J. Stöhr, R. Nakajima, A. Carl, M.G. Samant, C. Chappert, R. Mégy, P. Beauvillain, P. Veillet, G.A. Held, Microscopic origin of magnetic anisotropy in Au/Co/Au probed with X-ray magnetic circular dichroism, Phys. Rev. Lett. 75 (20) (1995) 3753–3755.
[22] J. Bansmann, S. Baker, C. Binns, J. Blackman, J.-P. Bucher, J. Dorantes-Dávila, V. Dupuis, L. Favre, D. Kechrakos, A. Kleibert, K.-H. Meiwes-Broer, G.M. Pastor, A. Perez, O. Toulemonde, K.N. Trohidou, J. Tuaillon, Y. Xie, Magnetic and structural properties of isolated and assembled clusters, Surf. Sci. Rep. 56 (2005) 189–275.
[23] O. Fruchart, Epitaxial self-organization: from surfaces to magnetic materials, C. R. Physique 6 (1) (2005) 61–73.
[24] O. Fruchart, Self-organization on surfaces: foreword, C. R. Physique 6 (1) (2005) 3–9.
[25] M. Albrecht, U. Gradmann, T. Furubayashi, W.A. Harrison, Magnetic moments in rough Fe surfaces, Europhys. Lett. 20 (1) (1992) 65–70.
[26] W. Weber, C.H. Back, A. Bischof, C. Würsch, R. Allenspach, Morphology-induced oscillations of the magnetic anisotropy in ultrathin Co films, Phys. Rev. Lett. 76 (1996) 1940–1943.
[27] A. Dallmeyer, C. Carbone, W. Eberhardt, C. Pampuch, O. Rader, W. Gudat, P. Gambardella, K. Kern, Electronic states and magnetism of monoatomic Co and Cu wires, Phys. Rev. B 61 (8) (2000) R5133–R5136.
[28] P. Gambardella, A. Dallmeyer, K. Maiti, M.C. Malagoli, S. Rusponi, P. Ohresser, W. Eberhardt, C. Carbone, K. Kern, Oscillatory magnetic anisotropy in one-dimensional atomic wires, Phys. Rev. Lett. 93 (7) (2004) 077203.
[29] P. Gambardella, Magnetism in monatomic metal wires, J. Phys.: Condens. Matter 15 (S2533–S2546).
[30] P. Gambardella, A. Dallmeyer, K. Maiti, M.C. Malagoli, W. Eberhardt, K. Kern, C. Carbone, Ferromagnetism in one-dimensional monoatomic metal chains, Nature 416 (2002) 301–304.
[31] P. Gambardella, S. Rusponi, M. Veronese, S.S. Dhesi, C. Grazioli, A. Dallmeyer, I. Cabria, R. Zeller, P.H. Dederichs, K. Kern, C. Carbone, H. Brune, Giant magnetic anisotropy of single cobalt atoms and nanoparticles, Science 300 (5622) (2003) 1130–1133.
[32] P. Gambardella, S. Rusponi, T. Cren, H. Brune, Magnetic anisotropy from single atoms to large monodomain islands on a metal surface, C. R. Physique 6 (1) (2005) 75–87.
[33] R. Guirado-López, J. Dorantes-Dávila, G. Pastor, Phys. Rev. Lett. 90 (2003) 226402.
[34] M. Jamet, W. Wernsdorfer, C. Thirion, D. Mailly, V. Dupuis, P. Mélinon, A. Pérez, Phys. Rev. Lett. 86 (2001) 4676–4679.
[35] A. Hubert, R. Schäfer, Magnetic Domains. The Analysis of Magnetic Microstructures, Springer, Berlin, 1999.
[36] M. Beleggia, M. De Graef, On the computation of the demagnetization tensor field for an arbitrary particle shape using a Fourier space approach, J. Magn. Magn. Mater. 263 (2003) L1–L9.
[37] E.C. Stoner, Philos. Mag. 36 (1945) 803.
[38] P. Rhodes, G. Rowlands, Demagnetizing energies of uniformly magnetized rectangular blocks, Proc. Leeds Philos. Liter. Soc. 6 (1954) 191.
[39] A. Aharoni, Demagnetizing factors for rectangular ferromagnetic prisms, J. Appl. Phys. 83 (6) (1998) 3432–3434.

[40] G. Rowlands, Ph.D. thesis, University of Leeds, Leeds, 1956.
[41] P. Rhodes, G. Rowlands, D.R. Birchall, J. Phys. Soc. Jpn. 17 (1956) 543.
[42] D.A. Goode, G. Rowlands, The demagnetizing energies of a uniformly magnetized cylinder with an elliptic cross-section, J. Magn. Magn. Mater. 267 (2003) 373–385.
[43] G. Rowlands, On the calculation of acoustic radiation impedance of polygonal-shaped apertures, J. Acoust. Soc. Am. 92 (5) (1992) 2961–2963.
[44] E.C. Stoner, E.P. Wohlfarth, A mechanism of magnetic hysteresis in heterogeneous alloys, Philos. Trans. Roy. Soc. London Ser. A 240 (1948) 599–642.
[45] A. Thiaville, Coherent rotation of magnetization in three dimensions: a geometrical approach, Phys. Rev. B 61 (18) (2000) 12221–12232.
[46] W. Wernsdorfer, Classical and quantum magnetization reversal studies in nanometer-sized particles and clusters, in: I. Prigogine, S.A. Rice (Eds.), in: Adv. Chem. Phys., vol. 118, Wiley, 2001, pp. 99–190.
[47] J.C. Slonczewski, Theory of magnetic hysteresis in films and its applications to computers, Research Memo RM 003.111.224, IBM Research Center, Poughkeepsie, NY, 1956.
[48] M. Lederman, S. Schultz, M. Ozaki, Phys. Rev. Lett. 73 (1994) 1986–1989.
[49] W.F. Brown Jr., Thermal fluctuations of a single-domain particle, Phys. Rev. 130 (1963) 1677–1686.
[50] C. Thirion, W. Wernsdorfer, D. Mailly, Nature Mater. 2 (2003) 524–527.
[51] C. Kittel, Phys. Rev. 70 (1946) 965–971.
[52] A. Aharoni, Introduction to the Theory of Ferromagnetism, Clarendon Press, Oxford, 1996.
[53] M.A. Schabes, H.N. Bertram, Magnetization processes in ferromagnetic cubes, J. Appl. Phys. 64 (3) (1988) 1347–1357.
[54] W. Rave, K. Fabian, A. Hubert, Magnetic states of small cubic particles with uniaxial anisotropy, J. Magn. Magn. Mater. 190 (1998) 332–348.
[55] R. Cowburn, D. Koltsov, A. Adeyeye, M. Welland, D. Tricker, Phys. Rev. Lett. 83 (1999) 1042–1045.
[56] R.P. Cowburn, M.E. Welland, Phase transitions in planar magnetic nanostructures, Appl. Phys. Lett. 72 (16) (1998) 2041–2043.
[57] W. Rave, A. Hubert, Magnetic ground state of a thin-film element, IEEE Trans. Magn. 36 (6) (2001) 3886.
[58] A. Aharoni, IEEE Trans. Magn. 27 (1991) 4775–4777.
[59] A. Thiaville, D. Tomáš, J. Miltat, Phys. Status Solidi A 170 (1998) 125–135.
[60] R.P. Cowburn, A.O. Adeyeye, M.E. Welland, Configurational anisotropy in nanomagnets, Phys. Rev. Lett. 81 (24) (1998) 5414–5417.
[61] R. Dittrich, A. Thiaville, J. Miltat, T. Schrefl, J. Appl. Phys. 93 (2003) 7891–7893.
[62] R.P. Cowburn, Property variation with shape in magnetic nanoelements, J. Phys. D: Appl. Phys. 33 (2000) R1–R16.
[63] Y. Nakatani, Y. Uesaka, N. Hayashi, Jpn. J. Appl. Phys. 28 (1989) 2485–2507.
[64] B. Yang, D. Fredkin, J. Appl. Phys. 79 (1996) 5755–5757.
[65] K. Kirk, M. Scheinfein, J. Chapman, S. McVitie, M. Gillies, B. Ward, J. Tennant, J. Phys. D: Appl. Phys. 34 (2001) 160–166.
[66] M. Grimsditch, A. Berger, J. Johnson, V. Metlushko, B. Ilic, P. Neuzil, R. Kumar, Magnetic stability of nano-particles: The role of dipolar instability pockets, Europhys. Lett. 54 (6) (2001) 813–819.
[67] O. Fruchart, J.-C. Toussaint, B. Kevorkian, Micromagnetic model of non-collective magnetization reversal in ultrathin magnetic dots with in-plane uniaxial anisotropy, Phys. Rev. B 63 (17) (2001) 174418.
[68] M. Eleoui, O. Fruchart, J.C. Toussaint, Micromagnetic model of magnetization reversal of magnetically hard ultrathin dots and stripes, J. Magn. Magn. Mater., in press.
[69] M. Dimian, H. Kachkachi, J. Appl. Phys. 91 (2002) 7625–7627.
[70] In preparation.
[71] R. Cowburn, D. Koltsov, A. Adeyeye, M. Welland, J. Appl. Phys. 87 (2000) 7067–7069.
[72] H.A.M. Van den Berg, A micromagnetic approach to the constitutive equation of soft-ferromagnetic media, J. Magn. Magn. Mater. 44 (1–2) (1984) 207–215.
[73] H.A.M. Van den Berg, Self-consistent domain theory in soft-ferromagnetic media. II. Basic domain structures in thin-film objects, J. Appl. Phys. 60 (1986) 1104.
[74] P. Bryant, H. Suhl, Thin-film magnetic patterns in an external field, Appl. Phys. Lett. 54 (1989) 78.
[75] P. Bryant, H. Suhl, Micromagnetic below saturation, J. Appl. Phys. 66 (1989) 4329.
[76] A. DeSimone, R.V. Kohn, S. Müller, F. Otto, R. Schäfer, Two-dimensional modelling of soft ferromagnetic films, Proc. Roy. Soc. London Ser. A 457 (2001) 2983–2991.
[77] R. Hertel, H. Kronmüller, Computation of the magnetic domain structure in bulk permalloy, Phys. Rev. B 60 (10) (1999) 7366–7378.
[78] P.O. Jubert, J.C. Toussaint, O. Fruchart, C. Meyer, Y. Samson, Flux-closure-domain states and demagnetizing energy determination in sub-micron size magnetic dots, Europhys. Lett. 63 (1) (2003) 135–141.
[79] O. Fruchart, J.C. Toussaint, P.-O. Jubert, W. Wernsdorfer, R. Hertel, J. Kirschner, D. Mailly, Angular-dependence of magnetization switching for a multi-domain dot: experiment and simulation, Phys. Rev. B 70 (2004) 172409, brief report.
[80] K.Y. Guslienko, V. Novosad, Y. Otani, H. Shima, K. Fukamichi, Field evolution of magnetic vortex state in ferromagnetic disks, Appl. Phys. Lett. 78 (24) (2001) 3848.
[81] K.Y. Guslienko, K.L. Metlov, Evolution and stability of a magnetic vortex in a small cylindrical ferromagnetic particle under applied field, Phys. Rev. B 63 (2001) 100403(R).
[82] P.-O. Jubert, R. Allenspach, Analytical approach to the single-domain-to-vortex transition in small magnetic disks, Phys. Rev. B 70 (2004) 144402.
[83] S. Cherifi, R. Hertel, J. Kirschner, H. Wang, R. Belkhou, A. Locatelli, S. Heun, A. Pavlovska, E. Bauer, Virgin domain structures in mesoscopic Co patterns: Comparison between simulation and experiment, J. Appl. Phys. 98 (2005) 043901.

[84] M. Hehn, K. Ounadjela, J.P. Bucher, F. Rousseaux, D. Decanini, B. Bartenlian, C. Chappert, Nanoscale magnetic domains in mesoscopic magnets, Science 272 (1996) 1782–1785.
[85] J.K. Ha, R. Hertel, J. Kirschner, Concentric domains in patterned thin films with perpendicular magnetic anisotropy, Europhys. Lett. 64 (6) (2003) 810–815.
[86] R. Hertel, O. Fruchart, S. Cherifi, P.-O. Jubert, S. Heun, A. Locatelli, J. Kirschner, Three-dimensional magnetic flux-closure patterns in mesoscopic Fe islands, Phys. Rev. B, in press.
[87] M. Schneider, H. Hoffmann, J. Zweck, Lorentz microscopy of circular ferromagnetic permalloy nanodisks, Appl. Phys. Lett. 77 (18) (2000) 2909–2911.
[88] Z.H. Wei, C.R. Chang, N.A. Usov, M.F. Lai, J.C. Wu, Evolution of vortex states under external magnetic field, J. Magn. Magn. Mater. 239 (2002) 1–4.
[89] M. Rahm, M. Schneider, J. Biberger, R. Pulwey, J. Zweck, D. Weiss, V. Umansky, Vortex nucleation in submicrometer ferromagnetic disks, Appl. Phys. Lett. 82 (23) (2003) 4110–4112.
[90] C.J. García-Cervera, Z. Gimbutas, W. E, Accurate numerical methods for micromagnetics simulations with general geometries, J. Comput. Phys. 184 (2003) 37–52.
[91] U. Hartmann, H.H. Mende, Hysteresis of Néel line motion and effective width of 180° Bloch walls in bulk iron, Phys. Rev. B 33 (7) (1986) 4777–4781.
[92] A. Thiaville, J. Miltat, Controlled injection of a singular point along a linear magnetic structure, Europhys. J. D 26 (1994) 57.
[93] A. Wachowiak, J. Wiebe, M. Bode, O. Pietzsch, M. Morgenstern, R. Wiesendanger, Direct observation of internal spin structure of magnetic vortex cores, Science 298 (2002) 577–580.
[94] T. Okuno, K. Shigeto, T. Ono, K. Mibu, T. Shinjo, MFM study of magnetic vortex cores in circular permalloy dots: behavior in external field, J. Magn. Magn. Mater. 240 (2002) 1–6.
[95] A. Thiaville, J.M. García, R. Dittrich, J. Miltat, T. Schrefl, Micromagnetic study of Bloch-point-mediated vortex core reversal, Phys. Rev. B 67 (2003) 094410.
[96] L. Piraux, J. George, J. Despres, C. Leroy, E. Ferain, R. Legras, K. Ounadjela, A. Fert, Appl. Phys. Lett. 65 (1994) 2484–2486.
[97] K. Nielsch, R. Wehrspohn, J. Barthel, J. Kirschner, U. Gösele, S. Fischer, H. Kronmüller, Hexagonally ordered 100 nm period nickel nanowire arrays, Appl. Phys. Lett. 79 (2001) 1360–1362.
[98] E. Snoeck, R. Dunin-Borkowski, F. Dumestre, P. Renaud, C. Amiens, B. Chaudret, P. Zurcher, Appl. Phys. Lett. 82 (2003) 88–90.
[99] E. Saitoh, H. Miyajima, T. Yamaoka, G. Tatara, Nature 432 (2004) 203–206.
[100] A. Thiaville, Y. Nakatani, Spin Dynamics in Confined Magnetic Structures III, Springer, Berlin, in press.
[101] R. McMichael, M. Donahue, IEEE Trans. Magn. 33 (1997) 4167–4169.
[102] Y. Nakatani, A. Thiaville, J. Miltat, J. Magn. Magn. Mater. 290–291 (2005) 750–753.
[103] M. Kläui, C. Vaz, J. Bland, L. Heyderman, F. Nolting, A. Pavlovska, E. Bauer, S. Cherifi, S. Heun, A. Locatelli, Appl. Phys. Lett. 85 (2004) 5637–5639.
[104] N. Schryer, L. Walker, J. Appl. Phys. 45 (1974) 5406–5421.
[105] H. Forster, T. Schrefl, W. Scholz, D. Suess, V. Tsiantos, J. Fidler, J. Magn. Magn. Mater. 249 (2002) 181–186.
[106] N. Vernier, D. Allwood, D. Atkinson, M. Cooke, R. Cowburn, Europhys. Lett. 65 (2004) 526–532.
[107] A. Yamaguchi, T. Ono, S. Nasu, K. Miyake, K. Mibu, T. Shinjo, Phys. Rev. Lett. 92 (2004) 077205.
[108] M. Kläui, P. Jubert, R. Allenspach, A. Bischof, J. Bland, G. Faini, U. Rüdiger, C. Vaz, L. Vila, C. Vouille, Phys. Rev. Lett. 94 (2005) 106601.
[109] S. Zhang, Z. Li, Phys. Rev. Lett. 93 (2005) 127204.
[110] A. Thiaville, Y. Nakatani, J. Miltat, Y. Suzuki, Europhys. Lett. 69 (2005) 990–996.
[111] P. Bruno, Geometrically constrained magnetic wall, Phys. Rev. Lett. 83 (12) (1999) 2425.
[112] O. Pietzsch, A. Kubetzka, M. Bode, R. Wiesendanger, Real-space observation of dipolar antiferromagnetism in magnetic nanowires by spin-polarized scanning tunneling spectroscopy, Phys. Rev. Lett. 84 (22) (2000) 5212–5215.
[113] L. Néel, Sur un nouveau mode de couplage entre les aimantations de deux couches minces ferromagnétiques, C. R. Acad. Sci. 255 (1962) 1676–1681.
[114] J.C.S. Kools, W. Cula, D. Mauri, T. Lin, Effect of finite magnetic film thickness on Néel coupling in spin valves, J. Appl. Phys. 85 (8) (1999) 4466–4468.
[115] J. Moritz, F. Garcia, J.C. Toussaint, B. Dieny, J.P. Nozières, Orange peel coupling in multilayers with perpendicular magnetic anisotropy: Application to (Co/Pt)-based exchange-biased spin-valves, Europhys. Lett. 65 (1) (2004) 123–129.
[116] H.A.M. Van den Berg, Physics and methods for studying metallic multilayers with interlayer exchange coupling and GMR response, in: Magnetic Multilayers and Giant Magneto-Resistance – Fundamentals and Industrial Applications, in: Springer Ser. Surface Sci., vol. 37, Springer, Heidelberg, 2000, pp. 179–262.
[117] P. Bruno, Theory of interlayer exchange interactions in magnetic multilayers, J. Phys.: Condens. Matter 11 (1999) 9403–9419.
[118] L. Thomas, M.G. Samant, S.S.P. Parkin, Domain-wall induced coupling between ferromagnetic layers, Phys. Rev. Lett. 84 (8) (2000) 1816–1819.
[119] L. Thomas, J. Lüning, A. Scholl, F. Nolting, S. Anders, J. Stöhr, S.S.P. Parkin, Oscillatory decay of magnetization induced by domain-wall stray fields, Phys. Rev. Lett. 84 (15) (2000) 3462–3465.
[120] J. Vogel, W. Kuch, R. Hertel, J. Camarero, K. Fukumoto, F. Romanens, S. Pizzini, M. Bonfim, F. Petroff, A. Fontaine, J. Kirschner, Influence of domain wall interactions on nanosecond switching in magnetic tunnel junctions, cond-mat/0509029.
[121] J.I. Martin, J. Nogués, K. Liu, J.L. Vicent, I.K. Schuller, Ordered magnetic nanostructures: fabrication and properties, J. Magn. Magn. Mater. 256 (2003) 449–501.

[122] N. Mikuszeit, E.Y. Vedmedenko, H.P. Oepen, Multipole interaction of polarized single-domain particles, J. Phys.: Condens. Matter 16 (2005) 9037–9045.
[123] O. Fruchart, J.-P. Nozières, W. Wernsdorfer, D. Givord, F. Rousseaux, D. Decanini, Enhanced coercivity in sub-micrometer-sized ultrathin epitaxial dots with in-plane magnetization, Phys. Rev. Lett. 82 (6) (1999) 1305–1308.
[124] T. Aign, P. Meyer, S. Lemerle, J.P. Jamet, J. Ferré, V. Mathet, C. Chappert, J. Gierak, C. Vieu, F. Rousseaux, H. Launois, H. Bernas, Magnetization reversal in arrays of perpendicularly magnetized ultrathin dots coupled by dipolar interaction, Phys. Rev. Lett. 81 (25) (1998) 5656–5659.
[125] J.I. Martin, J. Nogués, I.K. Schuller, M.J.V. Bael, K. Temst, C.V. Haesendonck, V.V. Moshchalkov, Y. Bruynseraede, Magnetization reversal in long chains of submicrometric Co dots, Appl. Phys. Lett. 72 (2) (1998) 225–257.
[126] I.D. Mayergoyz, Mathematical Models of Hysteresis, Springer-Verlag, New York, 1991.
[127] O. Henkel, Phys. Status Solidi 7919 (1964).
[128] S. Thamm, J. Hesse, The remanence of a Stoner–Wohlfarth particle ensemble as a function of the demagnetisation process, J. Magn. Magn. Mater. 184 (1998) 245–255.
[129] C. Vouille, A. Thiaville, J. Miltat, Thermally activated switching of nanoparticles: a numerical study, J. Magn. Magn. Mater. 272–276 (2004) e1237–e1238.
[130] E. Bonet-Orozco, W. Wernsdorfer, B. Barbara, A. Benoit, D. Mailly, A. Thiaville, Three-dimensional magnetization reversal measurements in nanoparticles, Phys. Rev. Lett. 83 (20) (1999) 4188–4191.
[131] Y. Lu, P.L. Trouilloud, D.W. Abraham, R. Koch, J. Slonczewski, S. Brown, J. Bucchignano, E. O'Sullivan, R.A. Wanner, W.J. Gallagher, Observation of magnetic switching in submicron magnetic-tunnel junctions at low frequency, J. Appl. Phys. 85 (8) (1999) 5267.
[132] W. Wernsdorfer, E. Bonet-Orozco, K. Hasselbach, A. Benoit, B. Barbara, N. Demoncy, A. Loiseau, H. Pascard, D. Mailly, Experimental evidence of the Néel–Brown model of magnetization reversal, Phys. Rev. Lett. 78 (9) (1997) 1791–1794.
[133] R. Victora, Phys. Rev. Lett. 63 (1989) 457–460.
[134] A. Thiaville, J. Magn. Magn. Mater. 182 (1998) 5–18.
[135] J. Kurkijärvi, Intrinsic fluctuations in a superconducting ring closed with a Josephson junction, Phys. Rev. B 6 (1972) 832.
[136] J. Ferré, Dynamics of the magnetization reversal: from continuous to patterned ferromagnetic films, in: Spin Dynamics in Confined Magnetic Structures, Springer, Heidelberg, 2001, pp. 127–160.
[137] J. Camarero, Y. Pennec, J. Vogel, M. Bonfim, S. Pizzini, M. Cartier, F. Ernult, F. Fettar, B. Dieny, Dynamical properties of magnetization reversal in exchange-coupled NiO/Co bilayers, Phys. Rev. B 64 (2001) 172402.
[138] J. Moritz, B. Dieny, J.P. Nozières, Y. Pennec, J. Camarero, S. Pizzini, Experimental evidence of a $1/H$ activation law in nanostructures with perpendicular magnetic anisotropy, Phys. Rev. B 71 (2005) 100402.
[139] S. Lemerle, J. Ferré, C. Chappert, V. Mathet, T. Giamarchi, P.L. Doussal, Domain wall creep in an ising ultrathin magnetic film, Phys. Rev. Lett. 80 (1998) 842–849.
[140] H.-B. Braun, Thermally activated magnetization reversal in elongated ferromagnetic particles, Phys. Rev. Lett. 71 (21) (1993) 3557–3560.
[141] H.B. Braun, Nucleation in ferromagnetic nanowires – magnetostatics and topology, J. Appl. Phys. 85 (8) (1999) 6172–6174.
[142] W.T. Coffey, P.J. Cregg, Y.P. Kalmykov, On the theory of Debye and Néel relaxation of single domain ferromagnetic particles, Adv. Chem. Phys. 83 (1993) 263.
[143] O. Fruchart, M. Klaua, J. Barthel, J. Kirschner, Self-organized growth of nanosized vertical magnetic pillars on Au(111), Phys. Rev. Lett. 83 (14) (1999) 2769–2772.
[144] P. Ohresser, N.B. Brookes, S. Padovani, F. Scheurer, H. Bulou, Magnetism of small Fe clusters on Au(111) studied by X-ray magnetic circular dichroism, Phys. Rev. B 64 (2001) 104429.
[145] S. Rusponi, T. Cren, N. Weiss, M. Epple, L. Claude, P. Buluschek, H. Brune, The remarkable difference between surface and step atoms in the magnetic anisotropy of 2D nanostructures, Nat. Mater. 2 (2003) 546.
[146] R.W. Chantrell, N.Y. Ayoub, J. Popplewell, The low field susceptibility of a textured superparamagnetic system, J. Magn. Magn. Mater. 53 (1985) 199–207.
[147] O. Fruchart, P.-O. Jubert, C. Meyer, M. Klaua, J. Barthel, J. Kirschner, Vertical self-organization of epitaxial magnetic nanostructures, J. Magn. Magn. Mater. 239 (2002) 224–227.
[148] O. Fruchart, Auto-organisation épitaxiale: des surfaces aux matériaux magnétiques, Habilitation, Institut National Polytechnique de Grenoble, 2003.
[149] Q. Pankhurst, J. Connolly, S.K. Jones, J. Dobson, Applications of magnetic nanoparticles in biomedicine, J. Phys. D: Appl. Phys. 36 (2003) R167–R181.
[150] R.P. Cowburn, M.E. Welland, Room temperature magnetic quantum cellular automata, Science 287 (2000) 1466–1468.
[151] H.J.G. Draaisma, W.J.M. de Jonge, Surface and volume anisotropy from dipole-dipolar interactions in ultrathin ferromagnetic films, J. Appl. Phys. 64 (7) (1988) 3610–3613.
[152] H. Dürr, S. Dhesi, E. Dudzik, D. Knabben, G. van der Laan, J. Goedkoop, F. Hillebrecht, Spin and orbital magnetization in self-assembled Co clusters on Au(111), Phys. Rev. B 59 (2) (1999) R701–R704.
[153] T. Koide, H. Miyauchi, J. Okamoto, T. Shidara, A. Fujimori, H. Fukutani, K. Amemiya, H. Takeshita, S. Yuasa, T. Katayama, Y. Suzuki, Direct determination of interfacial magnetic moments with a magnetic phase transition in Co nanoclusters on Au(111), Phys. Rev. Lett. 87 (2001) 257201.
[154] P. Gambardella, S.S. Dhesi, S. Gardonio, C. Grazioli, P. Ohresser, C. Carbone, Localized magnetic states of Fe, Co, and Ni impurities on alkali metal films, Phys. Rev. Lett. 88 (4) (2002) 047202.